# Local transformation leading to an efficient Fourier Modal Method for perfectly conducting gratings

Simon Félix,[1] Agnès Maurel,[2] and Jean-François Mercier[3]

[1]*LAUM, CNRS, Université du Maine, avenue Olivier Messiaen, 72085 Le Mans, France**

[2]*Institut Langevin, CNRS, ESPCI ParisTech, 1 rue Jussieu, 75005 Paris, France*

[3]*Poems, CNRS, ENSTA ParisTech, INRIA, 828 boulevard des Maréchaux, 91762 Palaiseau, France*

## Abstract

We present an efficient Fourier modal method for the wave scattering by perfectly conducting gratings (in the two polarizations). The method uses a geometrical transformation, similar to the one used in the C-method, which transforms the grating surface into a flat surface, thus avoiding to question the Rayleigh hypothesis; also, the transformation only affects a bounded inner region which naturally matches the outer region; this allows to apply a simple criterion to select the ingoing and outgoing waves. The method is shown to satisfy the reciprocity and the energy conservation and it has an exponential rate of convergence for regular groove shapes. Besides, it is shown that the size of the inner region, where the solution is computed, can be reduced to the groove depth, that is to the minimal computation domain.

*OCIS codes:* (050.0050) Diffraction and gratings; (000.4430) Numerical approximation and analysis. (050.1950) Diffraction gratings, (050.2770) Gratings, (260.2110) Electromagnetic optics

* Corresponding author: simon.felix@univ-lemans.fr

## 1. Introduction

Numerical methods to simulate the diffraction of waves by gratings have experienced successive improvements during the last decades. For penetrable gratings, the Fourier Modal Method, or Rigorous Coupled Wave analysis, has reached a high degree of accuracy and it is the most popular method being used today for modeling diffraction by penetrable gratings [1–8]. The case of impenetrable gratings, with Dirichlet boundary condition for Transverse Electric waves (TE) or with Neumann boundary condition for Transverse Magnetic waves (TM) is subject to more controversy. This is partially because many studies are concerned with the inspection of the Rayleigh hypothesis ([9–13] and [14], Chap. 10). In its original work [15], Rayleigh made the assumption that the scattered field inside the grooves can be expanded onto a series of waves moving away from the grating surface. This is *a priori* valid for shallow gratings, and much effort has been dedicated to inspect the range of validity of this hypothesis. In parallel to these studies, few works have proposed to use geometrical transformations which do not rely on the Rayleigh hypothesis. The so-called C-method has been proposed by Chandezon and co-workers in a series of papers [16–20]; it uses a translation coordinate system which transforms the grating surface into a plane surface. Following studies have presented a comparison of this method with classical ones, as the Rayleigh-Fourier method [21–23]. However, because the C-method uses a geometrical transformation that affects the whole space, applying the radiation condition may reveal difficult, since the selection of outgoing waves is not straightforward and requires eigensolutions to be determined. More recently, Shcherbakov and Tishchenko [24] introduced a geometrical transformation in some bounded region containing the grating, so that the new coordinates continuously match the natural Cartesian coordinates. This is to our opinion a key point that allows for natural matching to the outer region where the radiation condition has to be accounted for. Note that this concept of matching the outer region is of prime importance in geometrical (or optical) transformations as used for cloaking or say more generally wave control [25, 26]. In this paper, we use the same idea of a "local" geometrical transformation for impenetrable gratings. Otherwise, our proposed numerical scheme is similar to the Fourier Modal Method and it can be straightforwardly implemented.

A noticeable improvement of the presented method concerns the convergence, which is often not quantitatively reported in the literature. The convergence of a numerical method

for any problem is limited by the regularity of the computed field. For penetrable gratings, the wavefield has a discontinuous gradient, which limits the convergence of the method to a power law $N^{-3/2}$, $N$ being the truncation order of the Fourier, or modal, series [27]. If the limit of perfectly conducting grating is considered, the error in the Fourier method is known to increase but the convergence in terms of power law is the same; the shortcomings of the method, if any, may be due to a large error for low truncation or to the fact that the error enters in its power law decay for high truncation; we have not seen in the literature a representation of the error able to answer this question. In the present paper, these limiting cases are directly treated as impenetrable gratings and this modifies drastically the convergence. Indeed, our geometrical transformation leads to a modified wave equation in a continuously varying medium, with space-dependent coefficients having the same regularity than the groove profile. For smooth profiles (described by a function of class $C^\infty$), this produces a convergence with exponential rate, much better than the usual power laws.

The key steps of the presented method are 1) the geometrical transformation leading to a modified wave equation expressed in a bounded region of the space, 2) the introduction of an auxiliary field to get a system of coupled, first order differential equations, with simple boundary condition, 3) the modal expansions of the two wavefields leading to a usual system of evolution equations for the modal components. Steps 2 and 3 are similar to the $(E, H)$ formulation in the Fourier Modal Method. Finally, the modal components expressed in the virtual space do not question the Rayleigh hypothesis.

The paper is organized as follows. In Section 2, the modal formulation, Eq. (17), is derived. Section 3 is concerned with the numerical resolution. In the present paper, we use the impedance matrix, or the admittance matrix, (Sec. 3.A) and we implement a Magnus scheme, (Sec. 3.B). However, the Fourier Modal Method, based on the scattering matrix, would be as efficient to solve our system of coupled equations Eq. (17). In addition to illustrating examples, where the method is validated by comparison with a finite element code, we inspect in Section 4 the convergence of the method and the influence of the size of the transformed region, where the calculation is performed. Concluding remarks are collected in Section 5.

## 2. Modal formulation in the transformed space

We consider a perfectly conducting grating whose profile is described in the real space $(X, Y)$ by a periodic function $Y = f(X)$, with period $d$ (Fig. 1). The grating is illuminated from the vacuum ($Y > f(X)$) by a monochromatic plane wave with wavenumber $k$ and incidence angle $\theta$. A time dependence $e^{-i\omega t}$, $\omega$ the angular frequency, is understood throughout this paper, and it will be omitted in the following. The wave is polarized, either with the electric field parallel to the grooves: $\mathbf{E} = E(X, Y)\mathbf{e}_Z$, referred as Transverse Electric waves (TE), or with the magnetic field parallel to the grooves: $\mathbf{H} = H(X, Y)\mathbf{e}_Z$, referred as Transverse Magnetic waves (TM). For TE waves, a Dirichlet boundary condition is imposed at the surface of the perfectly conducting grating, while, for TM waves, a Neumann boundary condition applies.

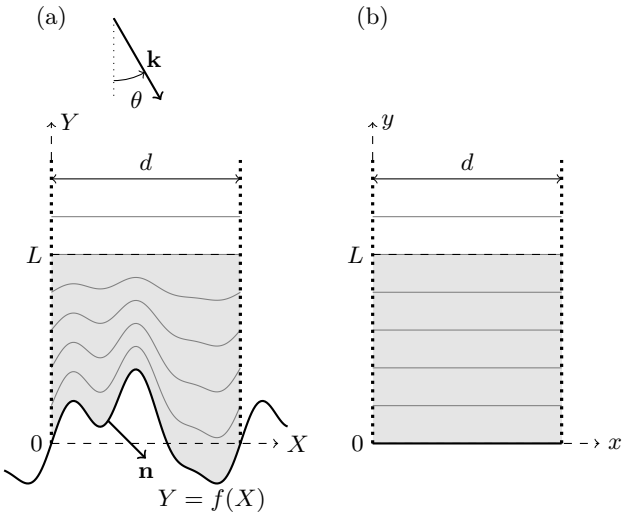


Fig. 1. (a) Grating in the real space with $(X, Y)$ coordinates, being $d$-periodic along $X$, illuminated by a wave (TE or TM) with wavenumber $\mathbf{k}$ at incidence $\theta$. The isolines of $y$-values resulting from the geometrical transformation, Eq. (4), are shown, with $y = 0$ on the grating surface and $y = L = Y$ being invariant. (b) Resulting virtual space in $(x, y)$ coordinates.

### 2.A. Geometrical transformation

The wavefield $u$, being either the electric field $u = E$ for TE waves or the magnetic field $u = H$ for TM waves, satisfies the Helmholtz equation

$$\left(\Delta + k^2\right) u = 0, \tag{1}$$

with periodic boundary conditions (respectively essential and natural b.c.)

$$u(d, Y) = e^{i\beta d} u(0, Y), \tag{2a}$$

$$\partial_X u(d, Y) = e^{i\beta d} \partial_X u(0, Y), \tag{2b}$$

and $\beta \equiv k \sin\theta$. On the grating surface $Y = f(X)$,

$$\begin{cases} u = 0 & \text{(Dirichlet b.c., in TE)}, \\ \mathbf{n} \cdot \nabla u = \partial_Y u - f' \partial_X u = 0 & \text{(Neumann b.c., in TM)}. \end{cases} \tag{3}$$

Next, we define a new coordinate system $(x, y)$ (transformed space) deduced from $(X, Y)$ in the real space:

$$\begin{aligned} x &\equiv X, \\ y &\equiv \begin{cases} L \dfrac{Y - f(X)}{L - f(X)}, & f(X) \le Y \le L \\ Y, & Y > L. \end{cases} \end{aligned} \tag{4}$$

The transformation is local, in the sense that for $Y > L$, the virtual and the real spaces coincide; this is of importance when the radiation condition will be taken into account. In practice, the numerical solution is computed in the transformed region $(0 \le y \le L)$ which corresponds to the region $(f(X) \le Y \le L)$ in the real space; we present below the calculations in that region.

### 2.B. Modified wave equation and boundary conditions

According to the theory of transformation media, mapping of the coordinates $(X, Y) \to (x, y)$ results in a change of the parameters appearing in the wave equation, Eq. (1). Denoting $\mathsf{J}$ the Jacobian tensor of the geometrical transformation, we obtain in the $(x, y)$ virtual space

$$\nabla \cdot \left( \frac{{}^t\mathsf{J}\mathsf{J}}{\det \mathsf{J}} \nabla u \right) + \frac{k^2}{\det \mathsf{J}} u = 0, \tag{5}$$

where the informations in the variable change (or metric informations) translate, for TE waves, in a new permeability tensor ${}^t\mathsf{J}\mathsf{J}/\det\mathsf{J}$ and a new permittivity $1/\det\mathsf{J}$ which vary in space (resp. a new tensor of permittivity and a new permeability for TM waves). Owing to Eq. (4), we get

$$\mathsf{J} = \begin{pmatrix} 1 & -a/b \\ 0 & 1/b \end{pmatrix}, \tag{6}$$

where

$$a(x,y) \equiv f'(x)\frac{L-y}{L}, \quad b(x) \equiv \frac{L-f(x)}{L}, \tag{7}$$

and with $\det\mathsf{J} = 1/b$,

$$\frac{{}^t\mathsf{J}\mathsf{J}}{\det\mathsf{J}} = \begin{pmatrix} b & -a \\ -a & (1+a^2)/b \end{pmatrix}. \tag{8}$$

Here, we have denoted $u(x,y) = u(X,Y)$ and $f(x) = f(X)$ in the virtual space to avoid multiple notations. The transformed wave equation Eq. (5) reads as

$$\partial_x\left(b\partial_x u - a\partial_y u\right) + \partial_y\left(-a\partial_x u + (1+a^2)/b\partial_y u\right) + k^2 b u = 0. \tag{9}$$

Next, rather than dealing with this second order equation on $u$, it is preferred to use coupled first order evolution equations along $y$. To do that, we use an auxiliary wavefield $v(x,y)$ defined as

$$v \equiv -a\partial_x u + \frac{(1+a^2)}{b}\partial_y u, \tag{10}$$

which is basically the quantity that is derived with respect to $y$ in Eq. (9). We get the desired coupled wave equations on $(u,v)$:

$$\begin{cases} \partial_y u &= \dfrac{ab}{1+a^2}\partial_x u + \dfrac{b}{1+a^2}v, \\ \partial_y v &= -bk^2 u - \partial_x\left(\dfrac{b}{1+a^2}\partial_x u\right) + \partial_x\left(\dfrac{ab}{1+a^2}v\right), \end{cases} \tag{11}$$

with the boundary conditions being translated in

$$u(d,y) = e^{i\beta d}u(0,y), \tag{12a}$$

$$\left[\partial_x u - \frac{a}{b}\partial_y u\right]_{x=d} = e^{i\beta d}\left[\partial_x u - \frac{a}{b}\partial_y u\right]_{x=0}, \tag{12b}$$

which means that $u$ and $\partial_x u$ are pseudo-periodic; then, at the grating surface $y = 0$, the boundary conditions for either TE or TM polarization, take the simple form

$$\begin{cases} u(x,0) = 0 & \text{(for Dirichlet b.c.)}, \\ v(x,0) = 0 & \text{(for Neumann b.c.)}. \end{cases} \tag{13}$$

### 2.C. Coupled modal wave equations

The fields $u(x,y)$ and $v(x,y)$ are now expanded as

$$\begin{cases} u(x,y) = \displaystyle\sum_{n=-\infty}^{+\infty} u_n(y)\varphi_n(x), \\ v(x,y) = \displaystyle\sum_{n=-\infty}^{+\infty} v_n(y)\varphi_n(x), \end{cases} \tag{14}$$

and here, the $\varphi_n(x)$ are chosen as

$$\varphi_n(x) = \frac{1}{\sqrt{d}} e^{i(\beta+2n\pi/d)x}, \tag{15}$$

to satisfy the pseudo-periodic boundary conditions. Note that the choice of the $\varphi_n$ as cosine or sine functions can be used straightforwardly to treat the case of waves propagating in Neumann or Dirichlet waveguides [27]. The common properties of the bases are the orthogonality relations

$$(\varphi_m, \varphi_n) = \delta_{mn} \quad \text{and} \quad (\varphi'_m, \varphi'_n) = \gamma_n^2 \delta_{mn}, \tag{16}$$

with $(f,g) = \int_0^d \mathrm{d}x \overline{f} g$ the scalar product. In the present case, we have $\gamma_n = \beta + 2n\pi/d$.

Let us stress again that, in our transformation, as in [16, 17, 24], the grating surface coincides with $y = 0$ which means that the expansion Eq. (14) does not question the Rayleigh hypothesis. This is because the modal components $u_n(y)$ are not equal to the modal components $u_n(Y)$ that would have been defined by expanding $u(X,Y)$ in the real space.

The projection of Eqs. (11) on the basis $\{\varphi_n\}$ leads to a set of first-order coupled equations governing the modal components $\mathbf{u} \equiv (u_n)$ and $\mathbf{v} \equiv (v_n)$:

$$\frac{\partial}{\partial y} \begin{pmatrix} \mathbf{u} \\ \mathbf{v} \end{pmatrix} = \begin{pmatrix} \mathsf{A}(y) & \mathsf{B}(y) \\ -k^2\mathsf{B}(L) + \mathsf{C}(y) & -\mathsf{A}^*(y) \end{pmatrix} \begin{pmatrix} \mathbf{u} \\ \mathbf{v} \end{pmatrix}, \tag{17}$$

with

$$\mathsf{A}_{mn} = \int_0^d \mathrm{d}x \, \frac{ab}{1+a^2} \overline{\varphi_m} \varphi'_n, \tag{18a}$$

$$\mathsf{B}_{mn} = \int_0^d \mathrm{d}x \, \frac{b}{1+a^2} \overline{\varphi_m} \varphi_n, \tag{18b}$$

$$\mathsf{C}_{mn} = \int_0^d \mathrm{d}x \, \frac{b}{1+a^2} \overline{\varphi'_m} \varphi'_n, \tag{18c}$$

and $\mathsf{A}^*$ the conjugate transpose of $\mathsf{A}$. Note that using the Bloch-Floquet modes (15), $\mathsf{C}$ is simply $\mathsf{C} = -\mathsf{\Gamma B \Gamma}$, with $\mathsf{\Gamma}$ the diagonal matrix given by $\mathsf{\Gamma}_m = i\gamma_m$.

## 3. Numerical Scheme

Several methods exist to solve the system of two coupled linear differential equations, Eq. (17). More often, it is solved using scattering matrix or reflection matrix methods which avoid the use of transfer matrix, known to produce numerical instabilities. Here, we present an alternative way based on the use of the impedance $\mathsf{Z}$ (or admittance $\mathsf{Y}$) matrix [27, 28].

### 3.A. Admittance/Impedance matrices

The impedance matrix $\mathsf{Z}$ links the two vectors $\mathbf{u}$ and $\mathbf{v}$ through $\mathbf{u} = \mathsf{Z}\mathbf{v}$. $\mathsf{Z}$ is known to satisfy a Riccati equation, from Eq. (17)

$$\mathsf{Z}' = \mathsf{B} + \mathsf{AZ} + \mathsf{ZA}^* + \mathsf{Z}\left[k^2\mathsf{B}(L) - \mathsf{C}\right]\mathsf{Z}, \tag{19}$$

which can be solved given an initial condition. For TE waves, $u = E$ vanishes at $y = 0$, leading to the initial condition $\mathsf{Z}(0) = 0$.

Since, for TM waves, the boundary condition at $y = 0$ is $v = 0$, Eq. (13), we rather use the admittance matrix $\mathsf{Y}$ which is the inverse of the impedance matrix, $\mathbf{v} = \mathsf{Y}\mathbf{u}$. Thus, it can be integrated with the initial condition $\mathsf{Y}(0) = 0$. In the following section, we present the Magnus scheme used to integrate the impedance/admittance matrix and, if needed, to compute the wavefield.

### 3.B. Magnus scheme

Basically, the coupled wave equations for the modal components, Eq. (17), are written formally as

$$\frac{\partial}{\partial y}\begin{pmatrix}\mathbf{u}\\ \mathbf{v}\end{pmatrix} = \mathsf{M}(y)\begin{pmatrix}\mathbf{u}\\ \mathbf{v}\end{pmatrix}, \tag{20}$$

and are solved using a Magnus scheme,

$$\begin{pmatrix}\mathbf{u}\\ \mathbf{v}\end{pmatrix}(y) = \exp\left[-\mathsf{M}(y + \mathrm{d}y/2)\mathrm{d}y\right]\begin{pmatrix}\mathbf{u}\\ \mathbf{v}\end{pmatrix}(y + \mathrm{d}y), \tag{21}$$

where the step size $\mathrm{d}y$ depends on the truncation order $N$ of the infinite series, that is using the expansions

$$u(x,y) = \sum_{n=-N}^{N} u_n(y)\varphi_n(x), \tag{22}$$

(same for $v$). Indeed, to capture the variations of the most evanescent mode considered in the truncation, typically $k_N = \sqrt{k^2 - \gamma_N^2} = i\alpha_N$, we fix $\mathrm{d}y = 1/\alpha_N$. We define the matrix $\mathsf{F}$

$$\begin{aligned} \mathsf{F}(y + \mathrm{d}y/2) &\equiv \exp\left[-\mathsf{M}(y + \mathrm{d}y/2)\mathrm{d}y\right] \\ &= \begin{pmatrix} \mathsf{F}_{11} & \mathsf{F}_{12} \\ \mathsf{F}_{21} & \mathsf{F}_{22} \end{pmatrix}, \end{aligned} \tag{23}$$

where each $\mathsf{F}_{ij}$ is a $(2N+1) \times (2N+1)$ matrix.

The problem is solved numerically in two steps, only the first of which is necessary to get the scattering properties. In the first step, only $\mathsf{Z}$ (or $\mathsf{Y}$) is calculated. To do that, we translate on $\mathsf{Z}$ the relations $\mathbf{u}(y) = \mathsf{F}_{11}\mathbf{u}(y + \mathrm{d}y) + \mathsf{F}_{12}\mathbf{v}(y + \mathrm{d}y)$ and $\mathbf{v}(y) = \mathsf{F}_{21}\mathbf{u}(y + \mathrm{d}y) + \mathsf{F}_{22}\mathbf{v}(y + \mathrm{d}y)$, where $\mathsf{F}$ is evaluated at $(y + \mathrm{d}y/2)$ to get

$$\mathsf{Z}(y + \mathrm{d}y) = \left[\mathsf{Z}(y)\mathsf{F}_{21} - \mathsf{F}_{11}\right]^{-1}\left[\mathsf{F}_{12} - \mathsf{Z}(y)\mathsf{F}_{22}\right] \tag{24}$$

and the integration is performed from $\mathsf{Z}(0) = 0$ to $\mathsf{Z}(L)$.

Similarly, for TM waves, the integration is performed from $\mathsf{Y}(0) = 0$ to $\mathsf{Y}(L)$ using

$$\mathsf{Y}(y + \mathrm{d}y) = \left[\mathsf{F}_{22} - \mathsf{Y}(y)\mathsf{F}_{12}\right]^{-1}\left[\mathsf{Y}(y)\mathsf{F}_{11} - \mathsf{F}_{21}\right]. \tag{25}$$

Accounting for the source term is easy when $\mathsf{Z}(L)$ or $\mathsf{Y}(L)$ is known. This is because, as in [13], the coordinate transform concerns only the bounded region $0 \leq y \leq L$. Thus, at the boundaries $y = L$ (and $Y = y \geq L$), the waves correspond to the physical, incident and reflected, waves in the real space; this has to be opposed to the C-method, where the physical incident and reflected waves have to be determined in the virtual space (being unbounded). We have thus, for $y \geq L$,

$$u(x,y) = e^{-ik\cos\theta y}\varphi_0(x) + \sum_{n=-N}^{N} R_n e^{ik_n(y-L)}\varphi_n(x), \tag{26}$$

and $v = \partial_y u$, leading to

$$\begin{cases} u_n(L) = e^{-ik\cos\theta L}\delta_{n0} + R_n, \\ v_n(L) = -ik\cos\theta e^{-ik\cos\theta L}\delta_{n0} + ik_n R_n, \end{cases} \tag{27}$$

from which the reflection coefficients $R_n$ (calculated at $y = L$) can be deduced by inversion of the relations

$$[ik_n\delta_{mn} - \mathsf{Y}_{mn}(L)]\, R_n = [ik\cos\theta\delta_{m0} + \mathsf{Y}_{m0}(L)]\, e^{-ik\cos\theta L}, \tag{28}$$

or

$$[ik_n\mathsf{Z}_{mn}(L) - \delta_{mn}]\, R_n = [ik\cos\theta\mathsf{Z}_{m0}(L) + \delta_{m0}]\, e^{-ik\cos\theta L}, \tag{29}$$

If the wavefield is looked for, it is sufficient to store the impedance matrix or the admittance matrix at each $y$. If so, the wavefield is calculated starting from the initial values $u_n(L)$ or $v_n(L)$ in Eq. (27); then, coming back to the Eq. (21), we use $\mathbf{u}(y) = \mathsf{F}_{11}\mathbf{u}(y + \mathrm{d}y) + \mathsf{F}_{12}\mathbf{v}(y + \mathrm{d}y)$ and $\mathbf{v}(y) = \mathsf{F}_{21}\mathbf{u}(y + \mathrm{d}y) + \mathsf{F}_{22}\mathbf{v}(y + \mathrm{d}y)$ to get, from $y = L$ to $y = 0$,

$$\mathbf{u}(y) = [\mathsf{F}_{11} + \mathsf{F}_{12}\mathsf{Y}(y + \mathrm{d}y)]\, \mathbf{u}(y + \mathrm{d}y), \tag{30}$$

or

$$\mathbf{v}(y) = [\mathsf{F}_{21}\mathsf{Z}(y + \mathrm{d}y) + \mathsf{F}_{22}]\, \mathbf{v}(y + \mathrm{d}y). \tag{31}$$

In the latter case, the wavefield $u(y)$ is deduced from $v(y)$ using $u(y) = Z(y)v(y)$.

### 3.C. Reciprocity, energy conservation

We check in this section that our formulation Eq. (17) satisfies the reciprocity relation and it conserves the energy. Reciprocity links two solutions $u_A$ and $u_B$ of the problem, namely

$$\nabla \cdot [u_A \nabla u_B - u_B \nabla u_A] = 0, \tag{32}$$

which translates, on our modal components, to

$$\partial_y \left[ {}^t\mathbf{u}_A \overline{\mathbf{v}}_B - {}^t\overline{\mathbf{u}}_B \mathbf{v}_A \right] = 0, \tag{33}$$

where we used that $u$ solution implies $\overline{u}$ solution (time reversal invariance of the Helmholtz equation). The energy conservation simply follows by choosing $\mathbf{u}_A = \mathbf{u}_B = \mathbf{u}$, leading to the conservation of the Poynting vector $\partial_y \Pi = 0$, with

$$\Pi(y) \propto \mathrm{Im}\left[ {}^t\overline{\mathbf{u}}\mathbf{v} \right]. \tag{34}$$

Since $\mathsf{B}$ and $\mathsf{C}$ are self-adjoint matrices, it follows directly that the reciprocity Eq. (33) and the energy conservation $\partial_y \Pi = 0$ are satisfied. In practice, the energy conservation is checked by inspecting the value of $|e-1|$,

$$e \equiv \sum_n |R_n|^2 \frac{k_n}{k\cos\theta}, \tag{35}$$

being the normalized reflected energy (with the notations of Eq. (26), and where the sum is performed with the propagating modes only); in all the presented results, the energy conservation has been found to be satisfied within $|e-1| \sim 10^{-11}$-$10^{-15}$.

## 4. Results

Before a more quantitative inspection of the numerical method, we report in Figures 2 examples of computed fields for complex shapes of the grating surface; in each case, the profiles are generated by summing sine and cosine functions ($d$-periodic, see figure caption); either TM polarization (Neumann b.c.) or TE polarization (Dirichlet b.c.) has been considered in the examples, and the non dimensional frequency $kd$ has been chosen such that the wavelength is of the same order than the grooves (a) and (b), much larger (rough surface type in (c)) and much smaller (d) . Note, in (b), the typical cat-eye pattern observed at the cut-off frequency and corresponding to the Rayleigh-Wood anomaly (see *e.g.* [14], Chap. 8). The modal calculation has been validated by comparison with a finite element code [29]; for the profile in Fig. 2(a), the difference between the computed fields is 9% with $N = 10$ and 1% with $N = 13$; for the profile in Fig. 2(b), at lower frequency, the difference between the computed fields is 10% with $N = 7$ and 1.5% with $N = 10$ .

In the following sections, we inspect the convergence of the method and the influence of the length $L$ of the transformed region in the case of a sine shape.

### 4.A. Convergence

The results on the convergence of the method have been obtained for a simple sine shape $f(x) = 0.5d(1-\cos 2\pi x/d)$, and $kd = 7.5\pi$, $\theta = \pi/4$. The modal components $u_n$ are shown to decrease exponentially with $n$ (Fig. 3(a)). This fast rate of decay is expected for infinitely differentiable $f(x)$ shapes. Indeed, this produces that all the coefficients in Eq. (9) are

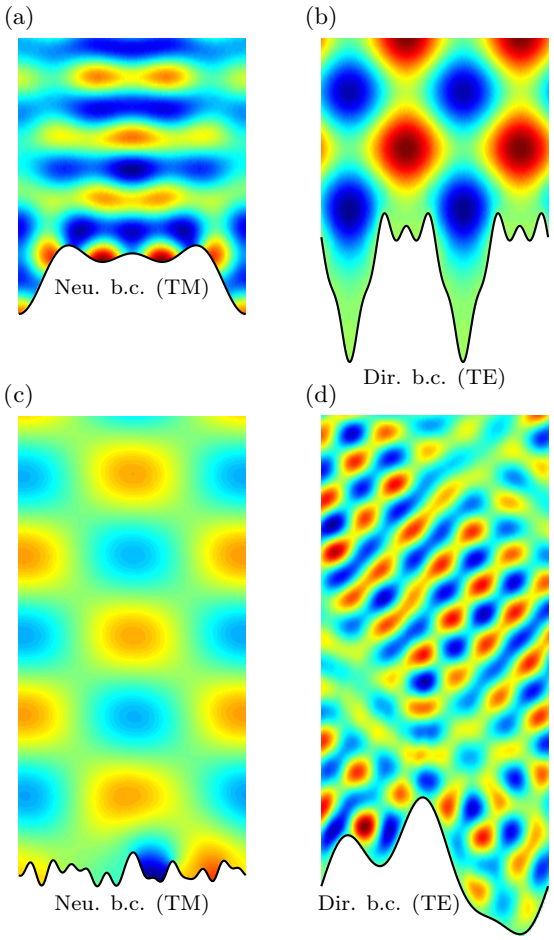


Fig. 2. Real part of the wavefield $u(x,y)$ for grating shapes $f(x) = \sum_p a_p \cos(2p\pi x/d) + b_p \sin(2p\pi x/d)$. (a) $\{a_p/d\}_{p=1,3} = [-0.08, -0.08, -0.06]$ (zero $b_p$) and $kd = 7.5\pi$, $\theta = 0$ (TM). (b) $a_2 = 0.25\ d$, $b_1 = -0.5\ d$, $b_5 = -0.1\ d$ (zero otherwise) and $kd = 2\pi$, $\theta = 0$ (TE) (c) For both $a_p$ and $b_p$: 15 values randomly chosen, $kd = 3.5\pi$, $\theta = -\pi/5$ (TM). (d) $\{a_p/d\}_{p=1,3} = [-0.13, 0.10, -0.04]$, $\{b_p/d\} = [0.19, 0.03, 0.07]$ and $kd = 10.5\pi$, $\theta = \pi/4$ (TE).

infinitely differentiable, hence $u$ and $v$ behave the same. Also, the $\varphi_n$-functions are adapted, which means here that they are pseudo-periodic (and all their derivatives). This behavior of the modal components produces an exponential convergence of the wavefield as well. This is illustrated in the Fig. 3(b), where we report the behavior of $\epsilon_N \equiv ||u - u^{ex}||/||u^{ex}||$, with $u$ the solution truncated at order $N$, Eq. (22), and where $u^{ex}$ refers to an exact solution (in practice, calculated for a large $N$-value). Note that the case of penetrable gratings would produce a convergence with a power law decay [27], because of the discontinuities in the contrasts between the two media; obviously, any power law is worse than the exponential

decay.

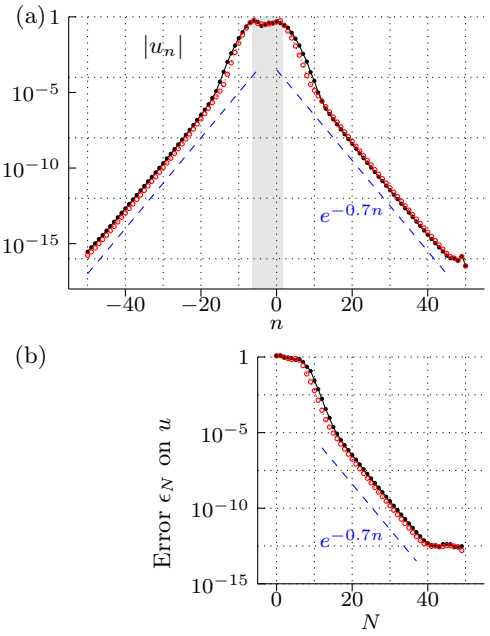


Fig. 3. (a) Rate of decay of the modal components $|u_n|$ (averaged over $y$); the gray strip indicates the $n$-values corresponding to propagating modes, (b) Convergence of the wavefield $|u|$ (averaged over $x$ and $y$ for $L = 2\max(f)$). In both Figures, for TM polarization (dotted lines with open symbols) and TE polarization (plain lines with closed symbols).

### 4.B. Influence of the size $L$ of the transformed region.

Figure 4 illustrates the fact that the calculated field does not depend on $L$, even in the limiting case where $L = \max(f)$ that is when only the grooves are resolved.

More quantitatively, we report in Fig. 5 the behavior of the reflection coefficient $R_0$ of the mode 0 for varying $L$-values; also the conservation of the energy given by $|e - 1|$, Eq. (35), is shown. For both TE and TM polarizations, small variations of $|R_0|$ are visible for $L$ in the range $[\max(f), 4\max(f)]$, whose amplitude decreases when increasing $N$. This fact, together with the fact that the energy is conserved even for $L = \max(f)$, shows that the calculation domain can be reduced to its minimum size (the groove thickness).

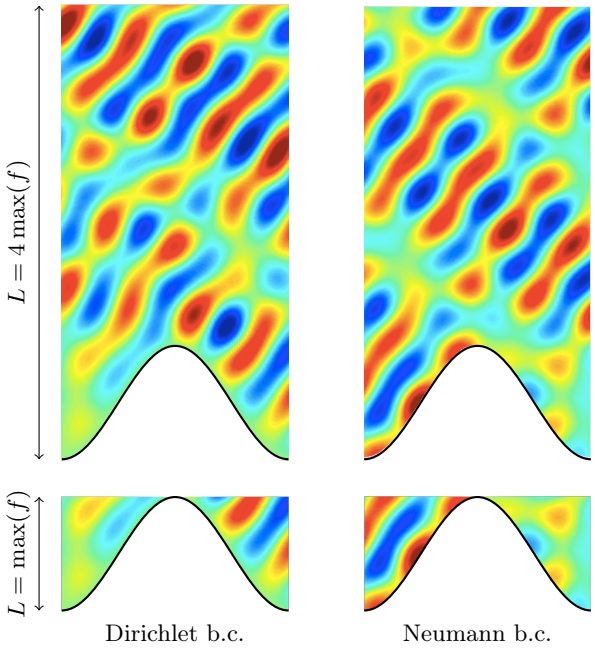


Fig. 4. Examples of computed fields for a sine shape $f(x) = a_0(1 - \cos 2\pi x/d)$, $a_0 = 0.25d$, $kd = 7.5\pi$, and $\theta = \pi/4$ ($\max(f) = 0.5d$). On bottom, for $L = \max(f)$ and on top for $L = 4\max(f)$.

### 4.C. A remark on profiles with discontinuous derivatives

Obviously, there is no restrictions to consider grating profiles with one of their derivatives being discontinuous; this is illustrated in Figure 6 for a profile with discontinuous first derivative and for a profile with discontinuous second derivative. In these cases, the convergence is degraded, from exponential decay to a power law decay ($\sim N^{-1}$ and $\sim N^{-3}$ for the given examples), as observed in other problems [27, 30]. Generally, we expect a power law convergence $N^{-\alpha}$, with $\alpha$ related to the regularity of the profile function (*e.g.*, to the order of the first discontinuous derivative). While increasing the regularity of the function, the exponential decay is progressively recovered.

However, the case of a profile with, locally, an infinite first derivative (*e.g.*, a discontinuous function $f(X)$) cannot be treated, though the multimodal equation (17) remains numerically workable. The Jacobian (6) becomes infinite if $f'$ is infinite, preventing a proper bijective coordinates change to be performed.

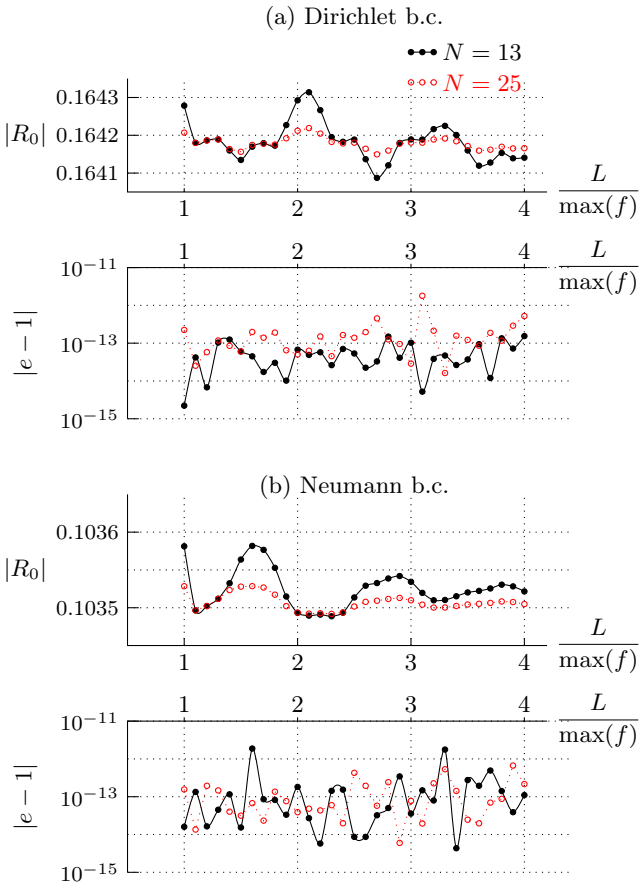


Fig. 5. Reflection coefficient $R_0$ as a function of $L$ for the configurations of Fig. 4 and $N = 13, 25$; energy conservation measured by $|e-1|$, see Eq. (35), as a function of $L$.

## 5. Conclusion

An efficient Fourier method is presented, for the scattering by perfectly conducting grating, either in TE or TM wave polarization. We use the idea of a geometrical transformation, introduced early in the C-method [16, 17], which transforms the grating surface into a plane surface, thus avoiding to question the Rayleigh hypothesis. Besides, as introduced recently in [24] for penetrable gratings, our transformation is local and continuously matches the outer region, which makes the radiation conditions easy to account for. The resulting system of coupled equations, Eq. (17), describes the wave propagation in the inner (rectangular) transformed region, and the space dependent coefficients encapsulate the complexity of the groove shape. Note that a Magnus scheme has been used to solve this system, but it could be solved equivalently using the Fourier Modal Method, FMM. The method has been validated

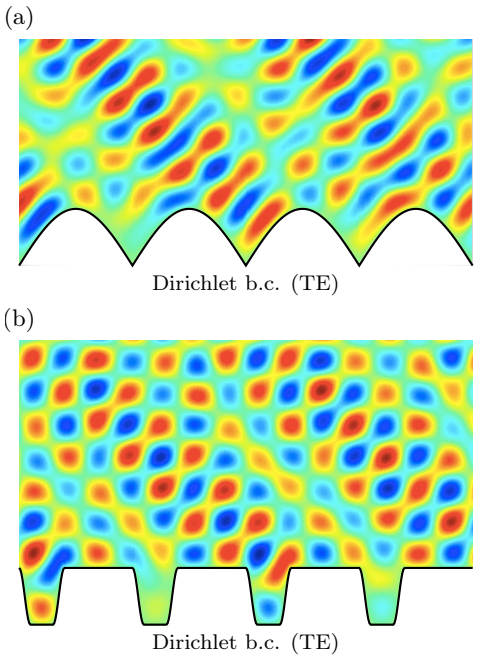


Fig. 6. Examples of wavefields for grating profiles having (a) a discontinuous first derivative and (b) a discontinuous second derivative.

by comparison with a finite element code, and it has been shown that it presents the following advantages: 1) it ensures reciprocity and energy conservation, 2) the inner region, where the calculations is performed, can be reduced to its minimum size, that is the thickness of the grooves, 3) the convergence of the method is exponential, which is the best expected convergence. Finally, a significant advantage of our formalism (not addressed in the present paper) is that it is well suited for perturbative calculations, as done in [31].

Note, finally, that the present method can be implemented straightforwardly in the case of wave propagating in waveguides, in 2D and 3D and this will be done elsewhere.

**Acknowledgments**

This work is supported by the Agence Nationale de la Recherche through the grant ANR ProCoMedia, project ANR-10-INTB-0914. A.M. acknowledge the financial support of the LABEX WIFI (Laboratory of Excellence within the French Program "Investments for the Future") under references ANR-10-LABX-24 and ANR-10-IDEX-0001-02 PSL*.

The authors thank G. Favraud and V. Pagneux for valuable discussions.

**References**


[1] M. G. Moharam and T. K. Gaylord, "Rigorous coupled-wave analysis of planar-grating diffraction", J. Opt. Soc. Am., **71**(7), 811-818 (1981).

[2] M. G. Moharam and T. K. Gaylord, "Rigorous coupled-wave analysis of grating diffraction - *E*-mode polarization and losses", J. Opt. Soc. Am., **73**(4), 451-455 (1983).

[3] P. Lalanne and G. M. Morris, "Highly improved convergence of the coupled-wave method for TM polarization", J. Opt. Soc. Am. A, **13**(4), 779-784 (1996).

[4] L. Li, "Use of Fourier series in the analysis of discontinuous periodic structures" J. Opt. Soc. Am. A, **13**(9), 1870-1876 (1996).

[5] E. Popov and M. Nevière, "Grating theory: new equations in Fourier space leading to fast converging results for TM polarization" J. Opt. Soc. Am. A, **17**(10), 1773-1784 (2000).

[6] E. Popov and M. Nevière, "Maxwell equations in Fourier space: fast-converging formulation for diffraction by arbitrary shaped, periodic, anisotropic media", J. Opt. Soc. Am. A, **18**(11), 2886-2894 (2001).

[7] G. Granet and B. Guizal, "Analysis of strip gratings using a parametric modal method by Fourier expansions", Opt. Com., **255**(1), 1-11 (2005).

[8] B. Guizal, H. Yala, and D. Felbacq, "Reformulation of the eigenvalue problem in the Fourier modal method with spatial adaptive resolution", Opt. Lett., **34**(18), 2790-2792 (2009).

[9] R.F. Millar, "The Rayleigh hypothesis and a related least squares solution to scattering problems for periodic surfaces and other scatterers", Radio Sc., **8**(8-9), 785-796 (1973).

[10] P.M. Van den Berg and J.T. Fokkema, "The Rayleigh hypothesis in the theory of reflection by a grating", J. Opt. Soc. Am., **69**(1), 27-31 (1979).

[11] T. Watanabe, Y. Choyal, K. Minami and V.L. Granatstein, "Range of validity of the Rayleigh hypothesis", Phys. Rev. E, **69**(5), 056606 (2004).

[12] J. Wauer and T. Rother, "Considerations to Rayleigh's hypothesis", Opt. Com., **282**(3), 339-350 (2009).

[13] A.V. Tishchenko, "Numerical demonstration of the validity of the Rayleigh hypothesis", Opt. Expr., **17**(19), 17102-17117 (2009).

[14] E.G. Loewen and E. Popov, Diffraction gratings and applications. CRC Press (1997).

[15] L. Rayleigh, "On the dynamical theory of gratings", Proc. R. Soc. Lond. A, **79**(532), 399-416

(1907).

[16] J. Chandezon, G. Raoult and D. Maystre, "A new theoretical method for diffraction gratings and its numerical application", J. Opt., **11**(4), 235-241 (1980).

[17] J. Chandezon, M. T. Dupuis, G. Cornet and D. Maystre, "Multicoated gratings: a differential formalism applicable in the entire optical region", J. Opt. Soc. Am., **72**(7) 839 -846 (1982).

[18] L. Li, G. Granet, J.P. Plumey and J. Chandezon, "Some topics in extending the C method to multilayer gratings of different profiles", Pure Appl. Opt., **5**(2) 141-146 (1996).

[19] L. Li, J. Chandezon, G. Granet and J.P. Plumey, "Rigorous and efficient grating-analysis method made easy for optical engineers", Appl. Opt., **38**(2), 304-313 (1999).

[20] A.Y. Poyedinchuk, Y.A. Tuchkin, N.P. Yashina, J. Chandezon and G. Granet, "C-method: Several aspects of spectral theory of gratings", Progress In Electromagnetics Research, **59**, 113-149 (2006).

[21] E. Popov and L. Mashev, "Convergence of Rayleigh-Fourier method and rigorous differential method for relief diffraction gratings", J. Mod. Opt., **33**(5), 593-605 (1986).

[22] T. Vallius, "Comparing the Fourier modal method with the C method: analysis of conducting multilevel gratings in TM polarization", J. Opt. Soc. Am. A, **19**(8), 1555-1562 (2002).

[23] K. Edee, J.P. Plumey and J. Chandezon, "On the Rayleigh-Fourier method and the Chandezon method: comparative study", Opt. Com., **286**, 34-41(2013).

[24] A. A. Shcherbakov and A.V. Tishchenko, "Efficient curvilinear coordinate method for grating diffraction simulation", Opt. Expr., **21**(21), 25236-25247 (2013).

[25] J. B. Pendry, D. Schurig, and D. R. Smith, Controlling electromagnetic fields, Science, **312**(5781), 1780-1782 (2006).

[26] N.I. Landy and W.J. Padilla, "Guiding light with conformal transformations", Opt. Exp., **17**(17), 14872-14879 (2009).

[27] A. Maurel, J.-F. Mercier and S. Félix, "Wave propagation through penetrable scatterers in a waveguide and though a penetrable grating", J. Acoust. Soc. Am. **135**(1), 165-174 (2014)

[28] V. Pagneux, "Multimodal admittance method in waveguides and singularity behavior at high frequencies", J. Comput. Appl. Math., **234**, 1834-1841 (2010).

[29] D. Martin, Melina Version 2.5 (2011), http://anum-maths.univ-rennes1.fr/-melina/danielmartin/melina/ (Last viewed: 2014/6/21).

[30] A. Maurel, J.-F. Mercier, and V. Pagneux, "Improved multimodal admittance method in

varying cross section waveguides", Proc. R. Soc. A, **470**, 20130448 (2014).

[31] A. Maurel, S. Félix, J.-F. Mercier, A. Ourir and Z.E. Djeffal, "Wood's anomalies for arrays of dielectric scatterers", J. Eur. Opt. Soc., **9**, 14001 (2014).